



Cite this: *Food Funct.*, 2022, **13**, 11840

## Okra (*Abelmoschus esculentus* L. Moench) prevents obesity by reducing lipid accumulation and increasing white adipose browning in high-fat diet-fed mice†

Heegu Jin,‡<sup>a</sup> Hyun-Ji Oh,‡<sup>a</sup> Sehaeng Cho,<sup>b,c</sup> Ok-Hwan Lee<sup>d</sup> and  
Boo-Yong Lee  \*<sup>a</sup>

Obesity is characterized by excessive fat accumulation owing to an imbalance between energy intake and expenditure. The suppression of lipid accumulation and the promotion of white adipose tissue (WAT) browning, which increases energy expenditure, may protect against obesity. Here, we demonstrate that okra complex (OKC) significantly reduces the body and WAT mass of mice by inhibiting adipogenesis and lipogenesis. We also show that OKC administration reduces fasting blood glucose and serum cholesterol and triglyceride (TG) concentrations and ameliorates liver steatosis in HFD-fed obese mice. In addition, OKC activates the protein kinase A (PKA) signaling pathway, which increases lipolysis; and induces the uncoupling protein 1 (UCP1)-mediated "browning" of WAT. These findings demonstrate that OKC has potentially beneficial effects on lipid metabolism and upregulates thermogenesis, which implies that it may be useful for the therapy and/or prevention of obesity and related metabolic diseases.

Received 20th September 2022,  
Accepted 25th October 2022

DOI: 10.1039/d2fo02790a  
[rsc.li/food-function](http://rsc.li/food-function)

## Introduction

Obesity is a major global health problem that is defined as a state of excessive adipose tissue accumulation caused by an imbalance in energy intake and expenditure.<sup>1</sup> Obesity can be associated with metabolic syndrome, a cluster of cardiovascular risk factors that include type 2 diabetes and hyperlipidemia, and is considered to be an important risk factor for non-alcoholic fatty liver disease (NAFLD).<sup>2,3</sup> Therefore, there is great interest in the prevention and treatment of obesity. White adipose tissue (WAT) plays an important role in lipid metabolism and the regulation of energy balance.<sup>4</sup> WAT stores excess energy in the form of triglyceride (TG), and can expand through increases in the number (hyperplasia) and/or size (hypertrophy) of adipocytes.<sup>5</sup>

Hyperplasia is the result of an upregulation of the ongoing process of the differentiation of preadipocytes into mature adipocytes, which is induced by the synergistic effects of adipogenic transcription factors, including CCAAT/enhancer-binding protein alpha (C/EBP $\alpha$ ), peroxisome proliferator-activated receptor gamma (PPAR $\gamma$ ), and fatty acid-binding protein 4 (FABP4).<sup>6</sup> In addition, lipid accumulation occurs during adipogenesis as a result of stimulation by lipogenic factors, including lysophosphatidic acid acyltransferase theta (LPAAT $\theta$ ), lipin 1, and diacylglycerol acyltransferase 1 (DGAT1).<sup>7</sup> Both adipogenesis and lipogenesis have been targeted for the treatment of obesity and obesity-related metabolic disease.<sup>8</sup>

The quantity of TG in adipocytes is regulated by both lipogenesis and lipolysis.<sup>9</sup> High levels of expression of lipogenic factors in adipocytes lead to the synthesis of TGs, whereas lipolysis is the degradation of TG to yield free fatty acids (FFAs) and glycerol.<sup>10</sup> The hydrolysis of TG is induced by the phosphorylation of protein kinase A (PKA), which in turn causes the transcription of genes encoding lipolytic enzymes.<sup>11</sup> Increasing PKA activity results in phosphorylation and regulated several key lipolytic proteins that account for TG lipase activity in adipocytes.<sup>12</sup> Adipose triglyceride lipase (ATGL) is the primary lipase for the initial step in hydrolyzing TG to form diglyceride (DG) and FFA; then PKA phosphorylation also promotes phosphorylated hormone-sensitive lipase (p-HSL)

<sup>a</sup>Department of Food Science and Biotechnology, College of Life Science, CHA University, Seongnam, Gyeonggi 13488, Republic of Korea

<sup>b</sup>Sysspang Co. Ltd, Seoul 06211, Republic of Korea

<sup>c</sup>Yonsei Medical Clinic, Seoul 04379, Republic of Korea

<sup>d</sup>Department of Food Biotechnology and Environmental Science, Kangwon National University, Chuncheon 24341, Republic of Korea

† Electronic supplementary information (ESI) available. See DOI: <https://doi.org/10.1039/d2fo02790a>

‡ These authors contributed equally to this work.



hydrolyzes DG to produce monoglyceride (MG) and FFA; and finally, monoacylglycerol lipase (MGL) hydrolyzes MG to liberate a further FFA molecule and glycerol.<sup>13</sup> These lipolytic enzymes are major phosphorylation targets of PKA and are regulated in lipid droplets in a PKA-dependent manner to stimulate lipolysis.<sup>14</sup> Phosphorylation of PKA leads the lipolysis pathway that generates FFAs and the released FFAs are transported to other tissues in the circulation for use as an energy source or may be metabolized in adipose tissue mitochondria.<sup>15</sup>

Brown adipose tissue (BAT) is an energy-consuming tissue, and is thus a potential target for the prevention of obesity.<sup>16</sup> The expression of uncoupling protein 1 (UCP1) in the mitochondria of BAT permits its specialized function: to generate heat through the dissipation of the proton gradient along the mitochondrial inner membrane, leading to the uncoupling of fatty acid oxidation from ATP synthesis.<sup>17,18</sup> BAT thermogenesis has an important role in the maintenance of body temperature in smaller mammals.<sup>19</sup> However, WAT adipocytes can also be induced to differentiate into brown-like adipocytes, a process that is referred to as “browning” and requires the expression of peroxisome proliferator-activated receptor alpha (PPAR $\alpha$ ), PPAR $\gamma$  coactivator 1-alpha (PGC1 $\alpha$ ), PR domain-containing16 (PRDM16), and UCP1.<sup>20,21</sup> This phenotypic switch enables thermogenesis, and therefore the activation of WAT browning may represent an effective strategy for the treatment and/or prevention of obesity.<sup>22</sup>

Many efforts to treat obesity have focused on developing anti-obesity drugs. However, only a few drugs are available in the market for obesity treatment because they are difficult to develop and associated with numerous adverse side effects.<sup>23</sup> Therefore, the focus has been on alternative strategy for the development of plant-derived natural dietary anti-obesity products that are generally regarded as safe, with no side effects.<sup>24</sup> Okra (*Abelmoschus esculentus* L. Moench), also known as lady's finger, is a flowering plant of the mallow family that is native to Africa, but which is now grown in many countries.<sup>25,26</sup> It is valued for its edible pods, which are approximately 15–20 cm in length and are roughly pentagonal in cross-section. Among the various useful components contained in okra, the effects of various physiological activities are known to be attributed to quercetin and its derivatives.<sup>27</sup> The pods of the okra plant have nutritional value, but have also been reported to have value for the treatment of various diseases: recent studies have demonstrated anti-oxidative, anti-diabetic, anti-hyperlipidemic, and anti-fatigue effects.<sup>28–30</sup> It has also previously been shown that okra lowers the blood glucose and cholesterol concentrations of streptozotocin-induced diabetic rats.<sup>31</sup> However, it has not been determined whether okra has an anti-obesity effect. Therefore, in the present study, we aimed to characterize the effects of okra on lipid accumulation and WAT browning in high-fat diet (HFD)-fed obese mice and the 3T3-L1 adipocyte cell line. The findings suggest that okra can prevent obesity and related metabolic diseases, likely by reducing lipid accumulation and promoting WAT browning.

## Materials and methods

### Preparation of okra complex

The okra that we used in this study was OKC (okra complex, which was obtained from Syspang Co., Ltd (Seoul, Korea)). Okra powder was prepared from okra pods (*Abelmoschus esculentus* L. Moench) by cutting them into small pieces (5 mm thickness), soaking the pieces in water at 20 °C to remove the free sugars and off-taste ingredients of okra, draining for 10 min, hot-air drying at >70 °C for >5 h, and powdering. Following this, 19% inulin and 6% citric acid were added to the okra powder, which was then sieved to yield a fine powder (<1 mm), designated as OKC. Its total carbohydrate content was 37.5%, its protein content was 10.7%, its lipid content was 1.7%, its total fiber content was 37.6%, its ash content was 6.4%, and its sodium content was 0.0859%. The components of the okra powder were analyzed using a Waters 2695 Separation Module high-performance liquid chromatography (HPLC) system consisting of a Waters 996 Photodiode Array Detector (Waters, Milford, MA, USA). A Capcell Pak C18 column (250 × 4.6 mm, 5  $\mu$ m; Osaka Soda, Osaka, Japan) was used for chromatographic separation and the detection wavelength was set at 254 nm. The mobile phases were water containing 0.5% acetic acid (solvent A) and acetonitrile (solvent B). The mobile phase was run in gradient mode as follows: 0–5 min, 5% solvent B; 5–50 min, 20% solvent B; and 50–55 min, 5% solvent B. The flow rate was set at 1.0 mL min<sup>-1</sup> and the injection volume was 10  $\mu$ L. A representative HPLC chromatogram of OKC is shown in Fig. 1. Quercetin-3-O-gentioside and isoquercitrin, the index component of OKC, were successfully analyzed as their predominant peaks, which were functionally determined (1.49 ± 0.01 mg g<sup>-1</sup> quercetin-3-O-gentioside and 1.39 ± 0.01 mg g<sup>-1</sup> isoquercitrin).

### Animals and treatments

The animal studies were performed according to the criteria outlined in the “Guide for the Care and Use of Laboratory Animals” arranged by the National Academy of Science and published by the National Institutes of Health, and were approved by the Institutional Animal Care and Use Committee of CHA University (IACUC, Approval Number 200156). Four-week-old male ICR mice were purchased from Orient Bio (Seongnam, Korea) and housed in a temperature- and humidity-regulated facility under a 12 h light/dark cycle. After a 1-week period of adaptation, the mice were randomly allocated to four groups ( $n = 12$  per group): a chow diet (CD) group, a high-fat diet (HFD) group, a group fed HFD supplemented with oral OKC at 150 mg kg<sup>-1</sup> day<sup>-1</sup> (OKC150), or a group fed HFD supplemented at 450 mg kg<sup>-1</sup> day<sup>-1</sup> (OKC450). OKC was dissolved in distilled water and we administered OKC by oral gavage to each of the mice. The HFD contained 60 kcal% as fat (D12450B, Research Diets, NJ, USA) and the CD contained 10 kcal% as fat (D12450B, Research Diets, NJ, USA). Each diet was fed for 8 weeks. During the experimental period, the body mass and dietary intake of the mice were measured weekly. At the end of the experiment, the mice were terminally anesthe-



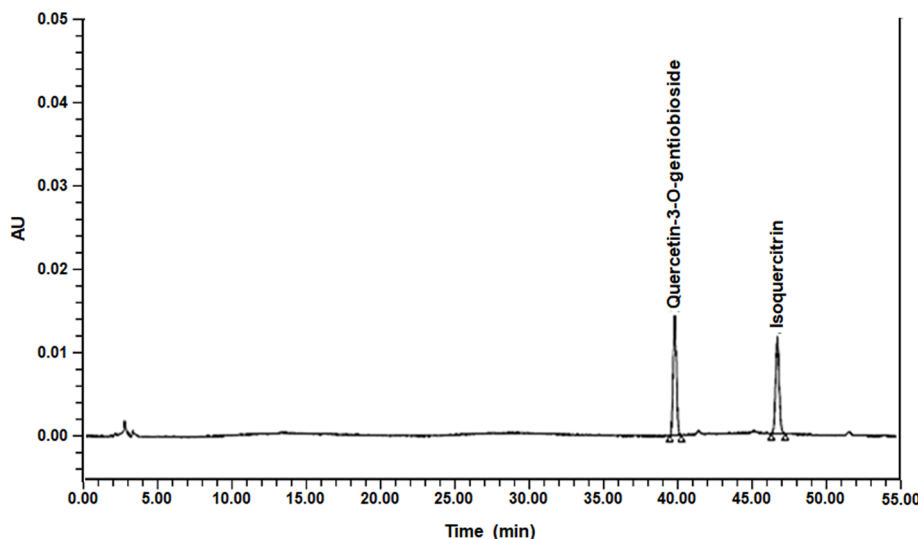


**Fig. 1** High-performance liquid chromatography (HPLC) chromatogram of okra complex (OKC).

tized with  $\text{CO}_2$  after fasting for 12 h, then blood and tissue samples were collected.

#### Fasting blood glucose measurement

The fasting glucose concentrations of blood samples collected weekly from a tail vein after 12 h of fasting were measured using an Accu-Check Blood Glucose Meter (Roche, Basel, Switzerland).

#### Oral glucose tolerance testing

Oral glucose tolerance testing (OGTT) was performed after an overnight fast. The mice were administered  $1.5 \text{ g kg}^{-1}$  body mass d-glucose orally, then the glucose concentrations of blood samples collected from a tail vein were measured after 0, 30, 60, 90, and 120 min using an Accu-Check Blood Glucose Meter.

#### Histological analysis

Subcutaneous (sWAT) and visceral (vWAT) WAT samples were fixed in 4% paraformaldehyde and embedded in paraffin. Multiple sections were then prepared and stained with hematoxylin and eosin (H&E) for histological evaluation. Photomicrographs were obtained using a Nikon E600 microscope (Nikon, Tokyo, Japan).

#### Rectal temperature measurement

The rectal temperatures of the mice were measured weekly using a Testo 925 Type Thermometer (Testo, Lenzkirch, Germany).

#### Immunofluorescence staining

WAT sections were deparaffinized and then incubated with anti-PKA or anti-UCP1 antibodies. Secondary anti-mouse fluorescein isothiocyanate (FITC)-conjugated and anti-rabbit Alexa Fluor<sup>TM</sup> 594-conjugated antibodies were then applied. DAPI

(Thermo Fisher Scientific, MA, USA) was used to stain the cell nuclei and the sections were mounted using ProLong Gold Antifade reagent (Thermo Fisher Scientific). Fluorescent images were captured using a Zeiss confocal laser scanning microscope (LSM880; Carl Zeiss, Oberkochen, Germany) and Zen 2012 software (Carl Zeiss).

#### Biochemical analysis

Blood samples were obtained by cardiac puncture under terminal anesthesia and centrifuged at  $3000\text{g}$  for 20 min at  $4^\circ\text{C}$  to collect serum. The serum concentrations of insulin were measured using a Mouse Metabolic Hormone Magnetic Bead Panel (Merck Millipore, Burlington, MA, USA). The serum concentrations of TG, total cholesterol, low-density lipoprotein (LDL)-cholesterol, and high-density lipoprotein (HDL)-cholesterol; and the activities of aspartate aminotransferase (AST) and alanine aminotransferase (ALT) were determined using colorimetric assay kits (Roche).

#### Cell culture

3T3-L1 preadipocytes were purchased from the American Type Culture Collection (Manassas, VA, USA) and cultured in Dulbecco's modified Eagle's medium (DMEM) containing 10% bovine calf serum (BS) and 1% penicillin/streptomycin (P/S) until confluent. After 2 days (D0), this medium was replaced with DMEM containing 10% fetal bovine serum (FBS), 1% P/S, and MDI (0.5 mM 3-isobutyl-1-methylxanthine, 1  $\mu\text{M}$  dexamethasone, and 4  $\mu\text{g mL}^{-1}$  insulin). On D2, this medium was replaced with DMEM containing 10% FBS, 1% P/S, and 4  $\mu\text{g mL}^{-1}$  insulin, and this was replaced every 2 days until day 8 (D8). For OKC treatment, 2-day confluent 3T3-L1 cells were incubated with different doses of OKC (0, 12, 25, 50, or 100  $\mu\text{g mL}^{-1}$ ) every 2 days during differentiation and until mature adipocyte formation (D8).



## Cell viability

To determine the appropriate concentrations of OKC to be used in further experiments, a cell viability assay was performed using 3-(4,5-dimethylthiazol-2-yl)-2,5-diphenyltetrazolium bromide (MTT, Thermo Fisher Scientific, Waltham, MA, USA). 3T3-L1 preadipocytes were seeded into 96-well plates and incubated overnight. Stock solutions of OKC were prepared in DMSO and then the cells were treated with various concentrations of OKC (0, 12, 25, 50, 100, or 200  $\mu\text{g mL}^{-1}$ ) for 24 h. MTT solution was added to each well, and the cells were incubated for a further 3 h. After removing the MTT-containing medium, DMSO was added to elute the formazan crystals. The absorbances of these eluates were then measured at 570 nm using a Bitek ELISA reader (BioTek, Winooski, VT, USA).

## Oil red O staining

After 8 days of 3T3-L1 cell differentiation, fully differentiated adipocytes were fixed in 4% formaldehyde for 1 h and washed twice with 60% isopropanol. The fixed cells were stained with Oil red O (ORO) solution for 30 min and then washed with distilled water. After drying, the stained cells were imaged and the stain was eluted using 100% isopropanol. To analyze hepatic lipid accumulation, cryostat sections of the liver were stained with ORO solution and photomicrographs were obtained.

## Western blot analysis

Tissues and cells were washed twice with PBS and then lysed in lysis buffer (1 mM phenylmethylsulfonyl fluoride, 1 mM ethylenediaminetetraacetic acid, 1  $\mu\text{M}$  pepstatin A, 1  $\mu\text{M}$  leupeptin, and 0.1  $\mu\text{M}$  aprotinin) (iNtRON Biotechnology, Seoul, Korea) containing phosphatase and protease inhibitors, and allowed to stand on ice for 1 h to permit lysis. After homogenization and centrifuge at 13 000g for 20 min at 4 °C, protein content in the supernatant was determined, and the lysate protein concentrations were quantified using a protein assay kit (Bio-Rad, Hercules, CA, USA). Lysates containing equal amounts of protein were separated using SDS-PAGE and the proteins were electrotransferred to membranes. Then, the membranes were blocked using 5% skim milk for 1 h, washed with Tris-buffered saline containing Tween 20 (TBST), incubated with primary antibodies overnight at 4 °C, and then exposed to horseradish peroxidase-conjugated secondary antibodies. Antibodies targeting C/EBP $\alpha$ , PPAR $\gamma$ , FABP4, sterol regulatory element-binding protein 1 (SREBP1), LPAAT $\theta$ , lipin 1, DGAT1, phosphorylated PKA (p-PKA, Ser 114), PGC1 $\alpha$ , and glyceraldehyde 3-phosphate dehydrogenase (GAPDH) were purchased from Santa Cruz Biotechnology (Dallas, TX, USA); antibodies targeting ATGL and phosphorylated HSL (p-HSL, Ser 563) were purchased from Cell Signaling Technology (Danvers, MA, USA); antibodies targeting MGL, PPAR $\alpha$ , PRDM16, and UCP1 were purchased from Abcam (Cambridge, UK); and an antibody targeting  $\beta$ -actin was purchased from ABM (Richmond, BC, Canada).

## Statistical analysis

Data are expressed as mean  $\pm$  SEM. Statistical comparisons were made using one-way ANOVA followed by Tukey's *post-hoc* test (IBM SPSS Statistics Version 20.0, Armonk, NY, USA).  $P < 0.05$  was regarded as indicating statistical significance.

## Results

### OKC inhibits HFD-induced obesity in mice

To determine the anti-obesity effects of OKC *in vivo*, we fed mice a CD, an HFD, or an HFD supplemented with 150 or 450 mg  $\text{kg}^{-1}$  day $^{-1}$  OKC for 8 weeks. At the end of this period, the HFD-fed mice were visibly larger than mice fed the CD, but mice in the OKC150 and OKC450 groups were dose-dependently thinner than those in the HFD group (Fig. 2A). As shown in Fig. 2B, OKC-treated mice were significantly protected from body mass gain during the 8 weeks of treatment, as a consequence of an OKC-induced reduction in WAT accumulation (Fig. 2C). Indeed, OKC significantly reduced the masses of the sWAT and vWAT (Fig. 2D), whereas the masses of other organs, such as the spleen, lung, and kidney, were unchanged (Fig. 2E). Thus, OKC reduced body mass, but did not cause substantial changes in food or water intake (Fig. 2F).

### OKC ameliorates hyperglycemia and dyslipidemia

We next assessed whether OKC ameliorates the HFD-induced glucose intolerance and insulin resistance. Over the 8 weeks of the experiment, the fasting blood glucose concentrations of the HFD group increased gradually, whereas they were significantly lower in the mice consuming the OKC, (Fig. 3A). As shown in Fig. 3B, the mice treated with OKC had better glucose tolerance at all the time points of the OGTT. Those consuming OKC showed a faster decline in blood glucose concentration and significantly lower serum insulin concentration than HFD-fed mice, implying an improvement in insulin sensitivity (Fig. 3C). In addition, OKC ameliorated the HFD-induced abnormalities in the serum lipid profile, including in TG, total cholesterol, LDL-cholesterol, and HDL-cholesterol concentrations (Fig. 3D-G). Thus, OKC ameliorates the hyperglycemia and dyslipidemia of HFD-fed mice.

### OKC consumption is associated with less adipogenesis and lipogenesis in WAT

The reductions in body and WAT mass, glucose intolerance, and dyslipidemia induced by OKC consumption were also associated with a reduction in the size of white adipocytes. As shown in Fig. 4A, H&E staining revealed that HFD-feeding led to adipocytes being much larger than CD-feeding. However, OKC-treated mice had smaller WAT adipocytes with less lipid accumulation (Fig. 4B). We also performed western blot analysis to determine the molecular mechanisms of the effects of OKC on adipocytes. The expression of key regulators of adipogenesis (C/EBP $\alpha$ , PPAR $\gamma$ , and FABP4) and lipogenesis (LPAAT $\theta$ , lipin1, and DGAT1) in both the sWAT and vWAT was significantly higher in the HFD group than in the CD group, consist-



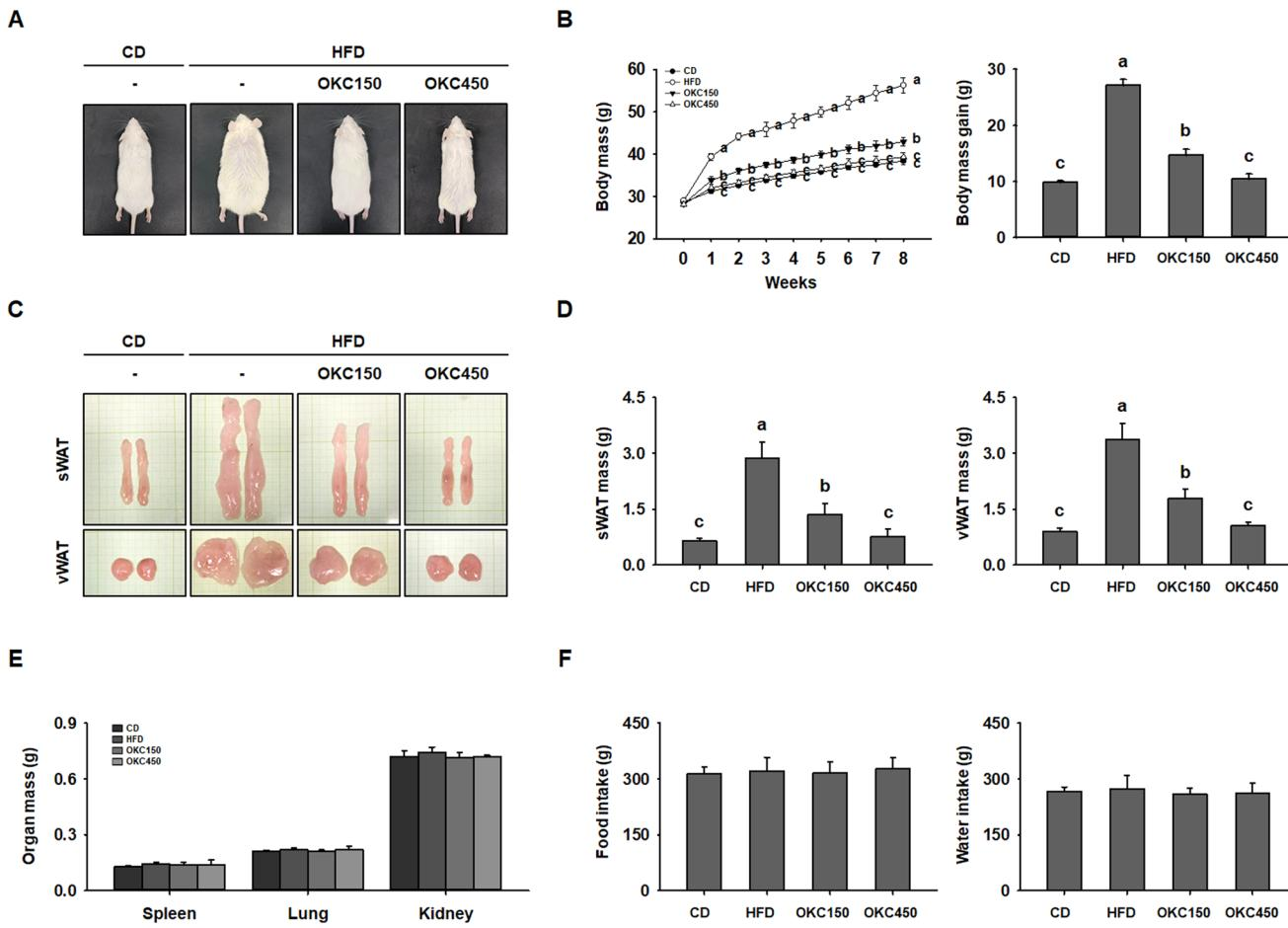


**Fig. 2** Effects of okra complex (OKC) on the obesity of high-fat diet (HFD)-fed obese mice. (A) Representative images of the mice after 8 weeks of feeding. (B) Body mass, measured regularly during the 8 weeks of OKC treatment. (C) Representative images of the subcutaneous (sWAT) and visceral (vWAT) adipose depots. (D) Masses of the sWAT and vWAT depots. (E) Masses of other organs. (F) Food and water intake during the 8 weeks of OKC treatment. Data are expressed as mean  $\pm$  SEM. Values with different letters are significantly different:  $p < 0.05$  (a > b > c).

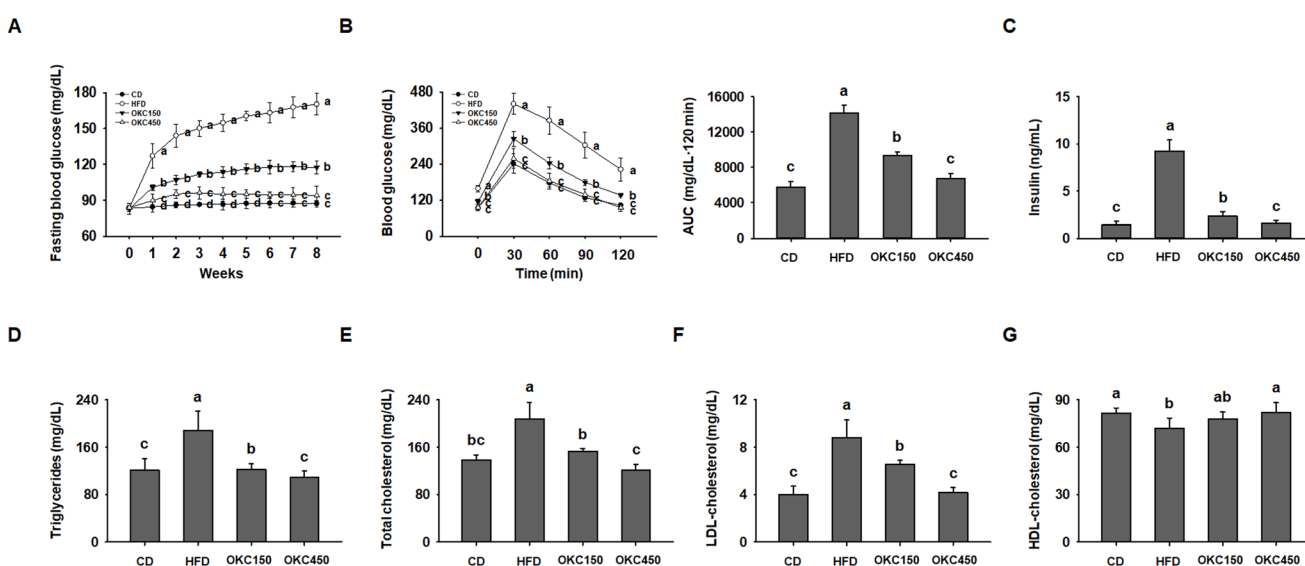


**Fig. 3** Effects of okra complex (OKC) on the hyperglycemia and dyslipidemia of HFD-fed mice. (A) Fasting blood glucose concentrations during the 8 weeks of OKC treatment. (B) Results of oral glucose tolerance testing after 8 weeks of OKC treatment: blood glucose concentrations at each time point and the areas under the curves (AUC). (C) Insulin, (D) triglyceride, (E) total cholesterol, (F) LDL-cholesterol, and (G) HDL-cholesterol concentrations after 8 weeks. Data are expressed as mean  $\pm$  SEM. Values with different letters are significantly different:  $p < 0.05$  (a > b > c > d).

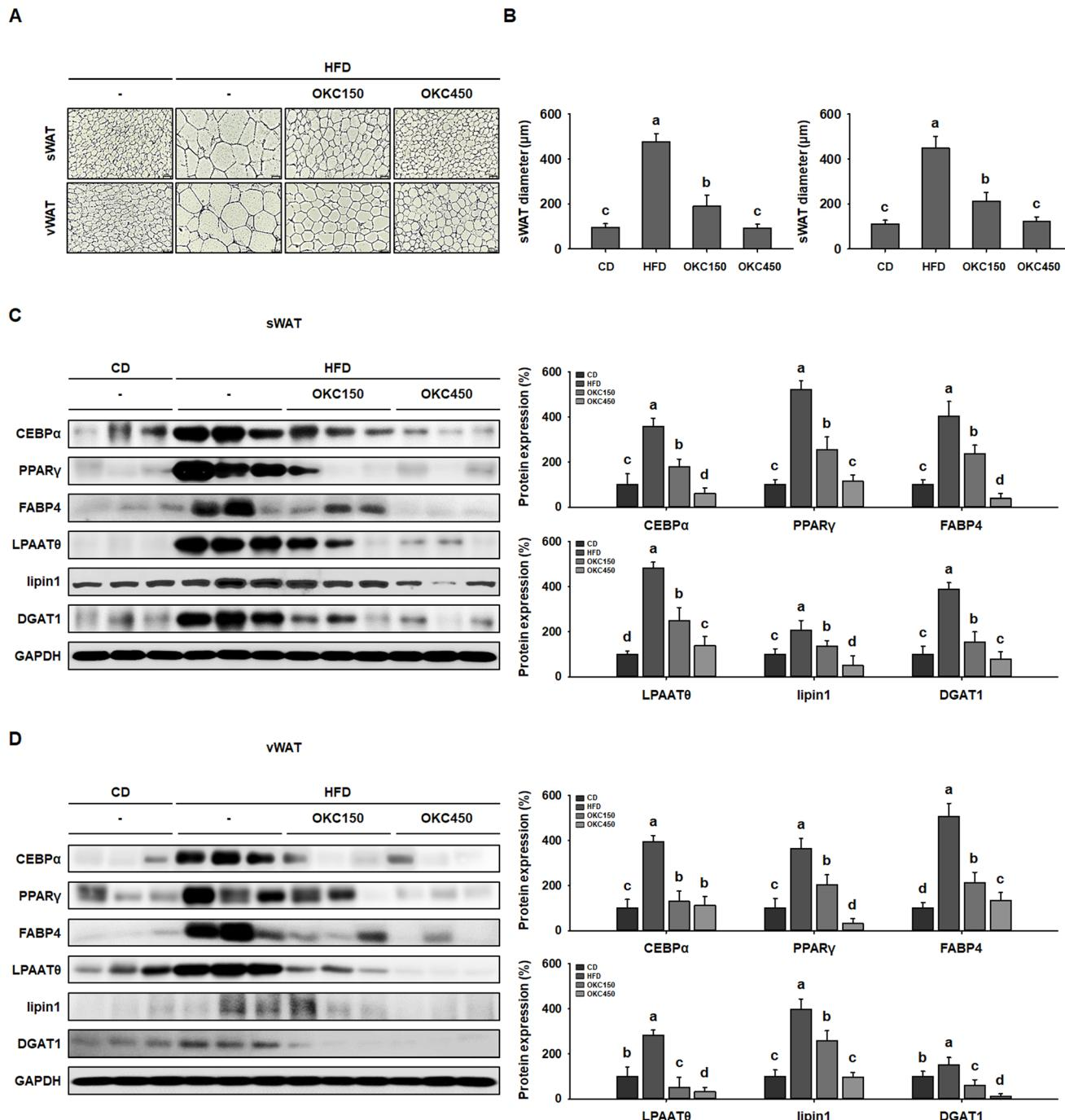


**Fig. 4** Effects of okra complex (OKC) on adipocyte size and the expression of adipogenic and lipogenic proteins in high-fat diet (HFD)-fed mice. (A) Sections of subcutaneous (sWAT) and visceral (vWAT) adipose tissue sections stained with hematoxylin and eosin. Scale bar: 100  $\mu$ m. (B) Diameters of adipocytes in the sWAT and vWAT depots. (C) Western blots of adipogenic proteins (CEBP $\alpha$ , PPAR $\gamma$ , and FABP4) and lipogenic proteins (LPAAT $\theta$ , lipin1, and DGAT1) in sWAT. (D) Western blots of adipogenic proteins (CEBP $\alpha$ , PPAR $\gamma$ , and FABP4) and lipogenic proteins (LPAAT $\theta$ , lipin1, and DGAT1) in vWAT. Data are expressed as mean  $\pm$  SEM. Values with different letters are significantly different:  $p < 0.05$  (a > b > c > d).

ent with the hypertrophy and hyperplasia of adipocytes that characterizes obesity. However, the expression of the adipogenic and lipogenic proteins was much lower in mice consuming OKC (Fig. 4C and D). These results imply that OKC inhibits adipogenesis and lipogenesis, reducing lipid accumulation in adipose depots.

#### OKC increases the expression of proteins involved in lipolysis and browning in WAT and increases body temperature

Greater lipolysis and the expression of UCP1 are characteristics of the browning of WAT.<sup>32</sup> To assess lipolysis in the WAT of the mice, we measured the phosphorylation of PKA and the

protein expression of ATGL, p-HSL, and MGL by western blot analysis, and found that OKC-treated mice had significantly higher expression of lipases and p-PKA than untreated HFD-fed mice, consistent with an upregulation of lipolysis (Fig. 5A and B). In addition, as shown in Fig. 5C and D, the HFD-fed

mice had lower body temperatures than the CD-fed mice, but the rectal temperatures of the OKC-treated mice were significantly higher than those of the other groups. This might be explained by greater dissipation of heat in WAT. Therefore, we measured the expression of proteins that mediate the brown-

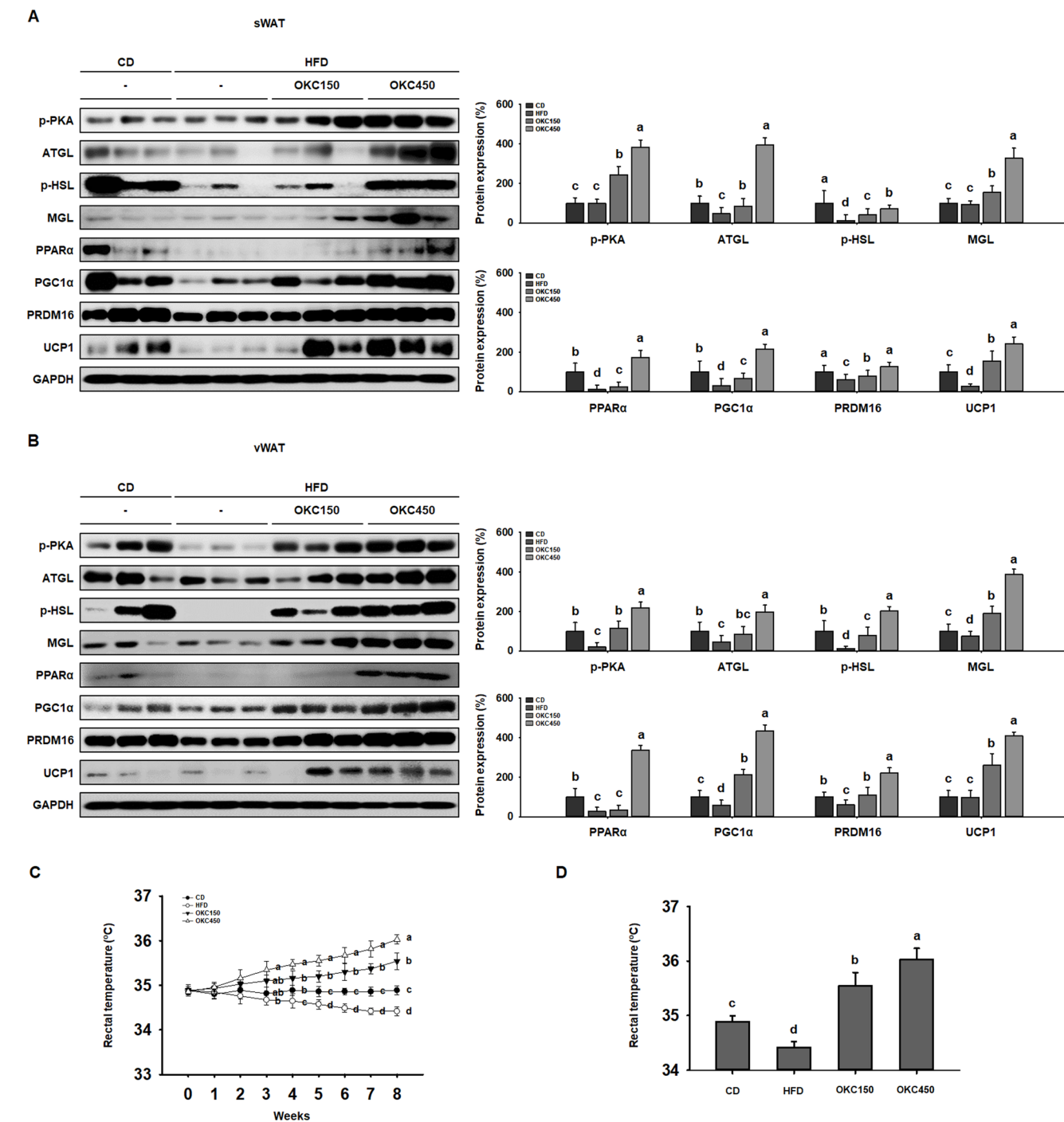


**Fig. 5** Effects of okra complex (OKC) on lipolysis and browning in the white adipose tissue (WAT) of high-fat diet (HFD)-fed mice. (A) Western blots of proteins involved in lipolysis (p-PKA, ATGL, p-HSL, and MGL) and browning (PPAR $\alpha$ , PGC1 $\alpha$ , PRDM16, and UCP1) in subcutaneous (s)WAT. (B) Western blots of proteins involved in lipolysis (p-PKA, ATGL, p-HSL, and MGL) and browning (PPAR $\alpha$ , PGC1 $\alpha$ , PRDM16, and UCP1) in visceral (v)WAT. (C) Rectal temperatures of the mice during 8 weeks of OKC treatment. (D) Rectal temperatures of the mice after 8 weeks of treatment. Data are expressed as mean  $\pm$  SEM. Values with different letters are significantly different:  $p < 0.05$  (a > b > c > d).



ing of WAT. As shown in Fig. 5A and B, OKC treatment induced the expression of the thermogenic genes PPAR $\alpha$ , PGC1 $\alpha$ , PRDM16, and UCP1 in the WAT of HFD-fed mice. Moreover, the intensity of immunofluorescence staining for PKA and UCP1 was higher in adipose tissue from OKC-treated mice (Fig. 6A and B). Taken together, these findings imply that OKC stimulates lipolysis and browning in WAT, resulting in greater loss of energy as heat.

### OKC ameliorates hepatic steatosis in the liver

HFD-feeding causes hepatic steatosis in the livers of obese mice.<sup>33</sup> Therefore, we next determined whether the hepatic lipid accumulation in HFD-fed mice was reduced by OKC. As shown in Fig. 7A, the livers of HFD-fed obese mice were yellowish-brown in color, but those of OKC-treated mice were a more normal reddish-brown color, similar to those of mice fed the CD. In addition, OKC significantly reduced the masses of the livers of HFD-fed mice (Fig. 7B). Next, we performed ORO staining of liver sections and found strong red staining of HFD-fed liver, confirming greater hepatic lipid droplet accumulation. However, OKC treatment significantly reduced the lipid content of the livers of HFD-fed mice (Fig. 7C). We also measured the serum AST and ALT activities and found that OKC reduced these (Fig. 7D and E). In addition, we measured the expression of hepatic lipogenic proteins (LPAAT $\theta$ , lipin1, DGAT1, and SREBP1) in mouse livers by western blot analysis. As shown in Fig. 7F, the HFD group showed high expression of these proteins, but OKC significantly reduced their expression, implying that OKC consumption limits hepatic lipid accumulation and the development of liver steatosis in HFD-fed mice.

### OKC suppresses lipid accumulation in 3T3-L1 cells

Next, to further investigate the mechanisms of the anti-obesity effects of OKC *in vitro*, we used 3T3-L1 adipocytes as a cell model. To assess the cytotoxicity of OKC, 3T3-L1 cells were treated with various concentrations, which did not cause a loss of cell viability up to 100  $\mu$ g mL $^{-1}$  (Fig. 8A). Therefore, 12, 25, 50, or 100  $\mu$ g mL $^{-1}$  OKC was used to determine how lipid accumulation is affected by OKC following the differentiation of 3T3-L1 cells. As shown in Fig. 8B, OKC inhibited adipocyte differentiation and reduced the number of intracellular lipid droplets. In addition, 3T3-L1 cells were stained with ORO solution, and this confirmed that OKC reduced lipid accumulation in a dose-dependent manner (Fig. 8C and D). These results demonstrate that OKC reduces lipid accumulation without having cytotoxic effects in 3T3-L1 adipocytes.

### OKC upregulates the expression of lipolytic and browning proteins in 3T3-L1 cells

To further investigate the molecular mechanisms whereby OKC affects the WAT phenotype, we performed western blot analysis of the expression of key proteins during 3T3-L1 differentiation. Consistent with the *in vivo* data, OKC treatment reduced adipogenic transcription factor expression in a dose-dependent manner (Fig. 9A) and significantly reduced the expression of lipogenic markers in 3T3-L1 cells (Fig. 9B). Because lipid accumulation in adipocytes was reduced by OKC treatment, we next evaluated whether OKC regulates lipolytic and browning protein expression in 3T3-L1 cells. As expected, and as shown in Fig. 9C, OKC increased the expression of lipolytic enzymes in a dose-dependent manner. Moreover, OKC markedly upregulated the expression of proteins involved in browning (Fig. 9D). Collectively, these results imply that OKC

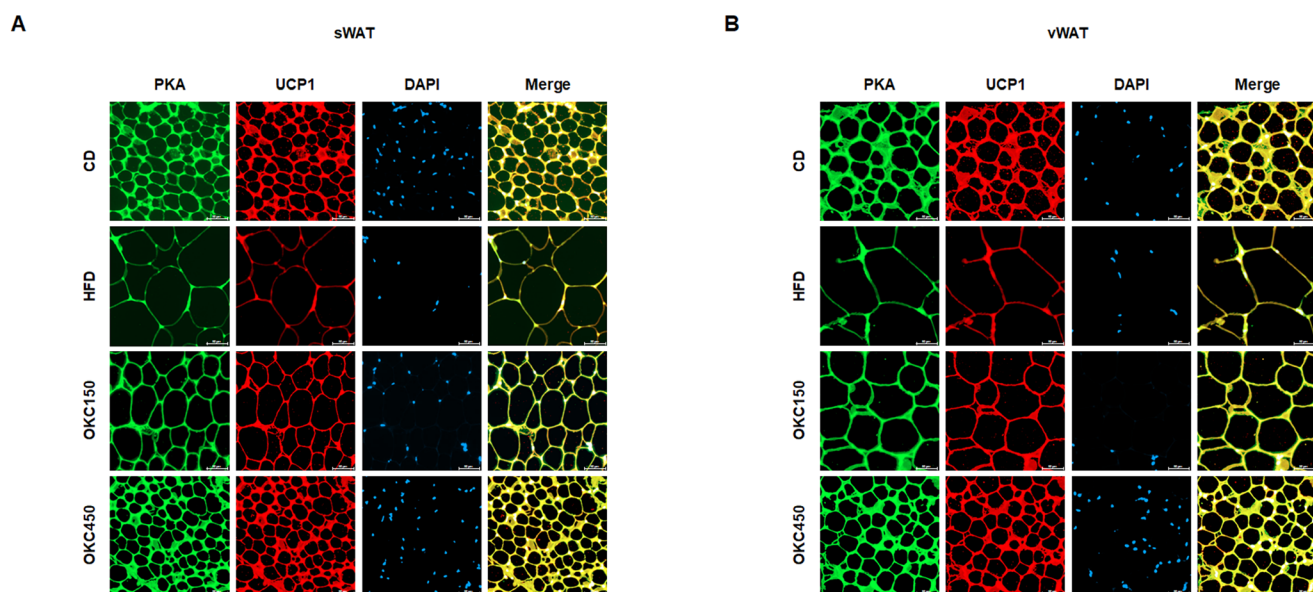


**Fig. 6** Double immunofluorescence staining of white adipose tissue (WAT) for lipolysis and browning. (A) Immunofluorescence images of the expression of PKA (green) and UCP1 (red) in sWAT and (B) vWAT (200 $\times$  magnification).



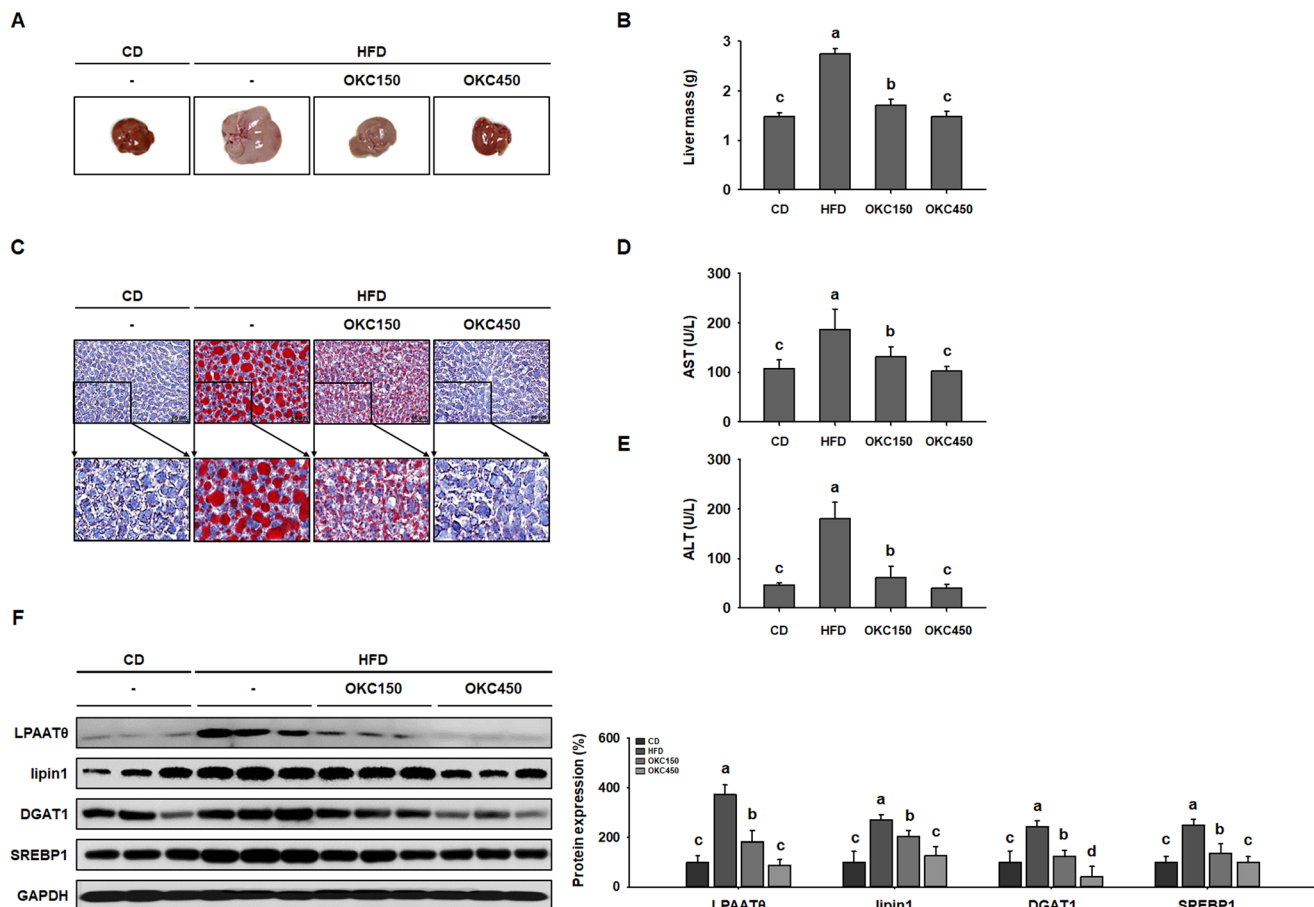


**Fig. 7** Effects of okra complex (OKC) on hepatic lipid accumulation in high-fat diet (HFD)-fed mice. (A) Representative images of mouse livers. (B) Liver masses. (C) Oil red O-stained liver sections from mice. Scale bar: 50 µm. (D) Serum AST and (E) ALT activities in HFD-fed mice. (F) Western blots of hepatic lipogenic protein expression (LPAAT0, lipin1, DGAT1, and SREBP1). Data are expressed as mean  $\pm$  SEM. Values with different letters are significantly different:  $p < 0.05$  (a > b > c > d).

reduces the expression of proteins involved in lipid accumulation and induces lipolysis and browning in 3T3-L1 adipocytes.

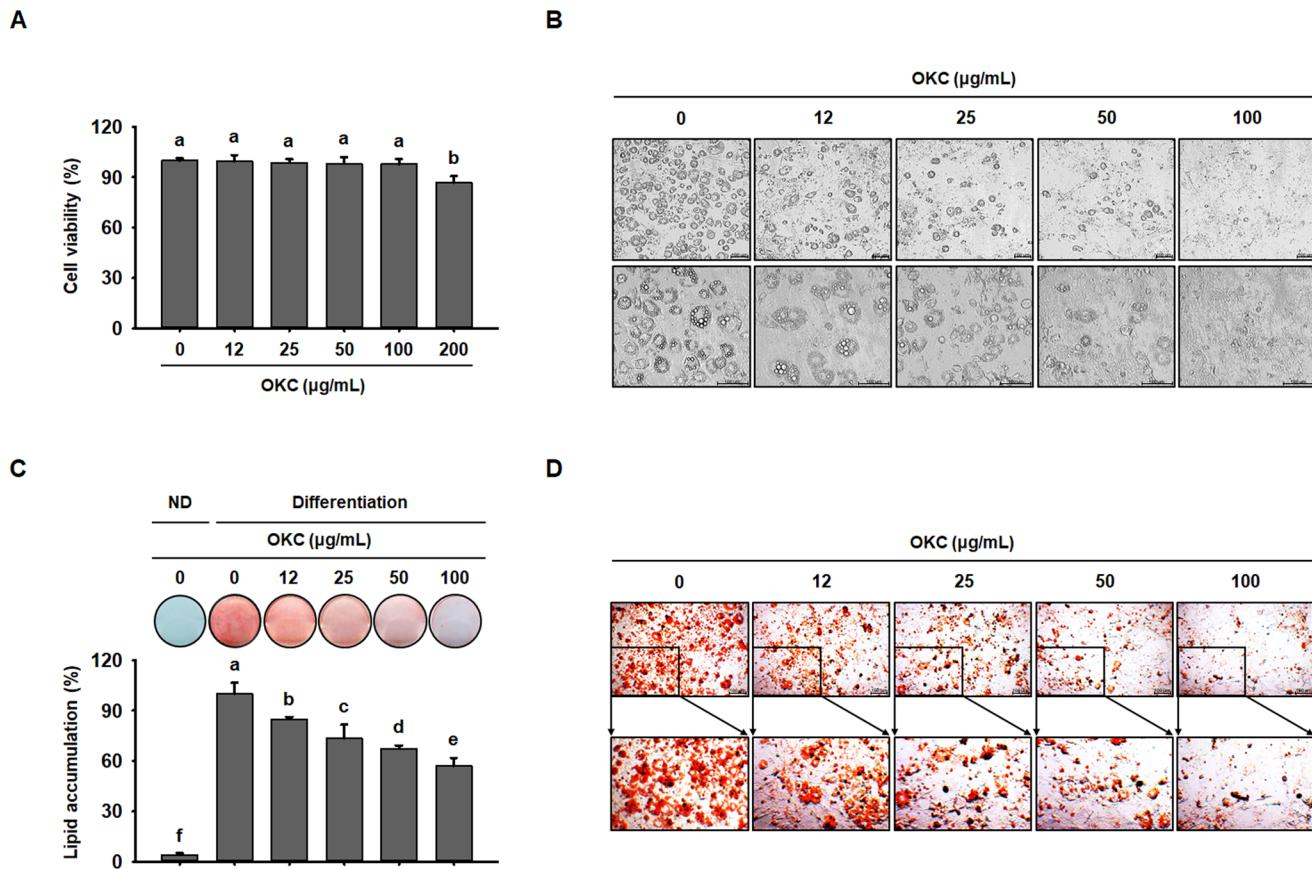
## Discussion

There has been great interest in the search for plant compounds that could be consumed and would reduce body mass and increase energy loss as a treatment for obesity and its related metabolic diseases.<sup>34,35</sup> In the present study, we evaluated the effects of OKC consumption on the obesity phenotype of HFD-fed mice. Okra, the major functional component of OKC, is a subfamily of dicotyledonous plants and contributes to anti-obesity activity (Fig. S1†). Recent studies have shown that okra reduces the circulating glucose and cholesterol concentrations in the diabetic state in rat,<sup>31</sup> but its effects on lipid accumulation and the browning phenotype in obesity have not been determined. To evaluate the potential anti-obesity effects of OKC, we determined the effects of OKC in HFD-fed obese mice and 3T3-L1 adipocytes. The results of the study suggest

that OKC not only reduces fat accumulation, but also induces energy expenditure, which is accompanied by improvements in overall metabolic status, in the form of glucose tolerance, serum lipid profile, and liver steatosis.

HFD-feeding is associated with high body mass and the excess accumulation of WAT.<sup>36</sup> As expected, mice fed an HFD for 8 weeks became obese, with significant increases in body mass and in the masses of both the SWAT and vWAT depots, which were accompanied by hyperglycemia and dyslipidemia. However, OKC consumption reduced the body and WAT masses, the fasting blood glucose concentration, and the serum insulin and lipid concentrations of the HFD-fed mice.

The observed differences in body mass and metabolic status were accompanied by differences in the size of WAT depots, which can be mediated through adipocyte hyperplasia and/or hypertrophy.<sup>37</sup> Hyperplasia involves the differentiation of adipocytes, mediated through the expression of adipogenic proteins (C/EBP $\alpha$ , PPAR $\gamma$ , and FABP4).<sup>38</sup> In addition, TG synthesis occurs, causing adipocyte hypertrophy, which requires high expression of lipogenic proteins (LPAAT0, lipin1, and DGAT1).<sup>39</sup> However, OKC reduced both the expression of both



adipogenic and lipogenic proteins, which explains the lower lipid accumulation in WAT. Thus, our data imply that OKC can prevent HFD-induced obesity by downregulating adipogenesis and lipogenesis.

Because obesity develops when energy intake consistently exceeds energy expenditure, increasing energy expenditure represents a strategy for the prevention of obesity.<sup>40,41</sup> The promotion of thermogenesis in WAT by inducing browning represents a much-researched specific potential strategy.<sup>42,43</sup> The lipolysis of TG to liberate FFAs and glycerol is necessary for WAT browning, and the released FFAs can be oxidized in mitochondria to generate heat.<sup>44</sup> Complete lipolysis requires a series of lipases and is regulated by PKA.<sup>45</sup> In the present study, we found that OKC induces the phosphorylation of PKA and increases the expression of the lipolytic enzymes ATGL, p-HSL, and MGL, which results in less TG storage in WAT. The FFAs released by PKA-induced lipolysis can be oxidized in browned WAT.<sup>46</sup>

As a first step to determine whether OKC induces WAT thermogenesis, we measured the body temperatures of the mice. HFD-fed mice had lower rectal body temperatures than CD-fed mice, but those of OKC-treated mice were higher than those of the other groups, which implies that OKC-treated mice main-

tain a higher level of thermogenesis even while consuming an HFD. We next assessed the browning phenotype of WAT, and found high expression of the thermogenic proteins PPAR $\alpha$ , PGC1 $\alpha$ , PRDM16, and UCP1 on western blots of WAT from OKC-treated mice, which means that OKC promotes WAT-to-BAT differentiation in WAT. Moreover, to determine whether OKC activates PKA and thus promotes UCP1, we performed immunofluorescence double staining. Consistent with this, the PKA and UCP1 immunoreactivities were higher in sections of adipose tissue from OKC-treated mice than in those from untreated HFD-fed mice. These results suggest that OKC increases lipolysis and causes the browning of WAT in HFD-fed mice, which probably implies that the body mass loss was due to an increase in energy expenditure, not due to physical activity or lower food intake and thus may mediate its anti-obesity effects.

HFD-feeding results in greater lipid synthesis, not only in WAT depots, but also in the liver, causing an accumulation of excessive amounts of TG, hepatic steatosis, and NAFLD in mice.<sup>47</sup> Mice fed the HFD showed substantial lipid accumulation in their livers, indicated by their yellow color and greater mass. However, OKC treatment near-normalized the color of the liver and reduced its mass. Consistent with this, ORO

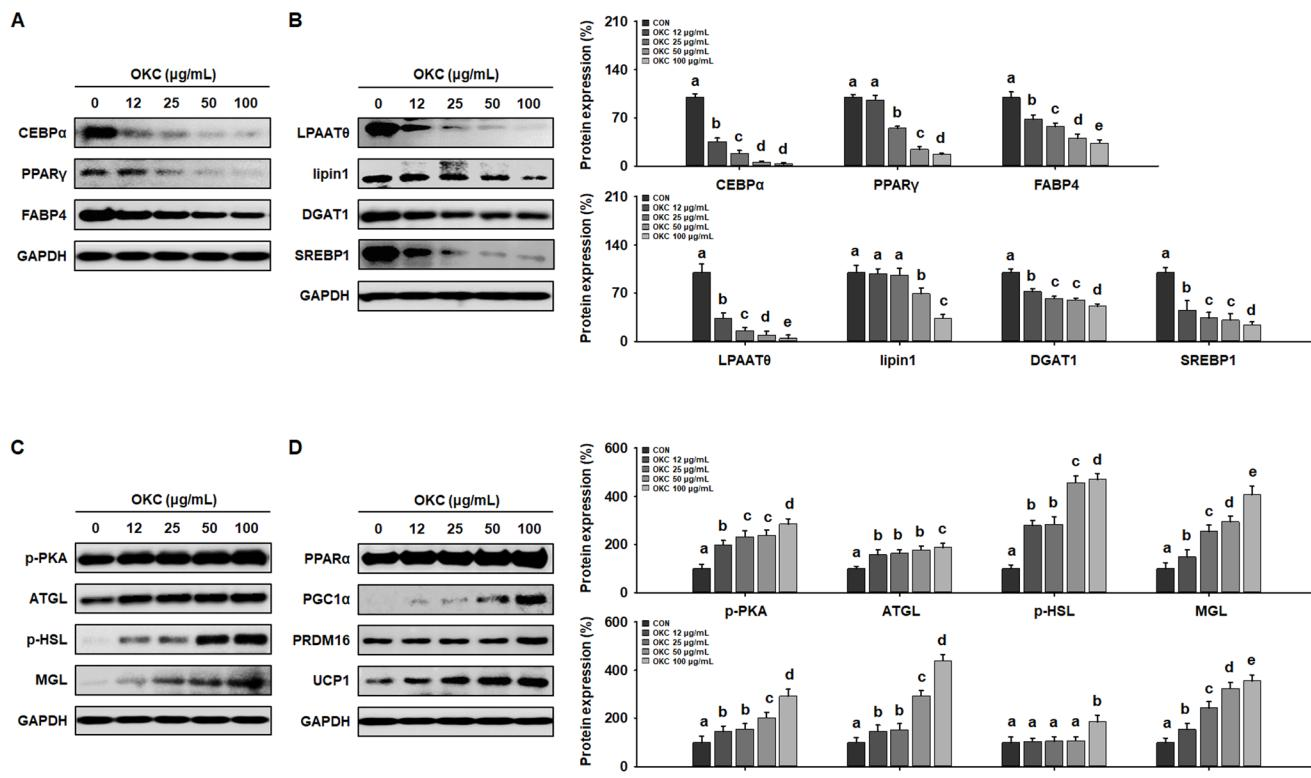


**Fig. 9** Effects of okra complex (OKC) on expression of proteins involved in lipid metabolism in differentiated 3T3-L1 cells. (A) Western blots of adipogenic proteins ( $\text{C/EBP}\alpha$ ,  $\text{PPAR}\gamma$ , and  $\text{FABP}4$ ) in 3T3-L1 cells. (B) Western blots of lipogenic proteins (LPAAT8, lipin1, DGAT1, and SREBP1) in 3T3-L1 cells. (C) Western blots of proteins involved in lipolysis (p-PKA, ATGL, p-HSL, and MGL) in 3T3-L1 cells. (D) Western blots of browning-related proteins (PPAR $\alpha$ , PGC1 $\alpha$ , PRDM16, and UCP1) in 3T3-L1 cells. Data are expressed as means  $\pm$  SEM. Values with different letters are significantly different:  $p < 0.05$  (a > b > c > d > e).

staining demonstrated that OKC significantly reduced hepatic TG accumulation and reduced the serum AST and ALT activities, consistent with less ongoing liver damage. Moreover, hepatic TG accumulation is mediated through the lipogenic proteins LPAAT8, lipin1, DGAT1, and SREBP1, the expression of which was reduced by OKC treatment. Therefore, OKC reduces lipid accumulation in the liver and ameliorates hepatic steatosis in HFD-fed mice.

The 3T3-L1 cell line is a well-established model of adipocyte differentiation and is widely used to study the browning of adipocytes.<sup>48</sup> Therefore, we also studied the effects of OKC using this model, and found that OKC inhibits lipid droplet accumulation by reducing the expression of proteins involved in adipogenesis and lipogenesis. In addition, OKC treatment increased the expression of proteins involved in lipolysis and browning in a dose-dependent manner, consistent with our *in vivo* findings.

## Conclusions

The present data show that the consumption of OKC reduces body mass gain and fat accumulation, and also improves the metabolic phenotype (hyperglycemia, dyslipidemia, and hepatic steatosis) of HFD-fed obese mice. These effects may be

mediated through greater lipolysis and browning of WAT. These findings suggest that OKC may represent a new means of treating obesity and its associated metabolic diseases.

## Author contributions

Heegu Jin: Conceptualization, methodology, software, validation, formal analysis, investigation, data curation, writing – original draft, writing – review & editing, visualization. Hyun-Ji Oh: Validation, data curation. Sehaeng Cho: Resources. Ok-Hwan Lee: Validation, project administration. Boo-Yong Lee: Conceptualization, resources, supervision, project administration, funding acquisition.

## Conflicts of interest

There are no conflicts to declare.

## References

- 1 N. V. Dhurandhar, What is obesity?, *Int. J. Obes.*, 2022, **46**, 1081–1082.

2 M. H. Ahmed, N. E. O. Husain and A. O. Almobarak, Nonalcoholic Fatty liver disease and risk of diabetes and cardiovascular disease: what is important for primary care physicians?, *J. Fam. Med. Prim. Care*, 2015, **4**, 45–52.

3 T. S. Han and M. E. Lean, A clinical perspective of obesity, metabolic syndrome and cardiovascular disease, *JRSM Cardiovasc. Dis.*, 2016, **5**, 2048004016633371–2048004016633371.

4 S. S. Choe, J. Y. Huh, I. J. Hwang, J. I. Kim and J. B. Kim, Adipose Tissue Remodeling: Its Role in Energy Metabolism and Metabolic Disorders, *Front. Endocrinol.*, 2016, **7**, 30–30.

5 J. Jo, O. Gavrilova, S. Pack, W. Jou, S. Mullen, A. E. Sumner, S. W. Cushman and V. Periwal, Hypertrophy and/or Hyperplasia: Dynamics of Adipose Tissue Growth, *PLoS Comput. Biol.*, 2009, **5**(3), e1000324.

6 S. R. Farmer, Transcriptional control of adipocyte formation, *Cell Metab.*, 2006, **4**, 263–273.

7 Y. J. Seo, H. Jin, K. Lee, J. H. Song, S. Chei, H. J. Oh, J. H. Oh and B. Y. Lee, Cardamonin suppresses lipogenesis by activating protein kinase A-mediated browning of 3T3-L1 cells, *Phytomedicine*, 2019, **65**, 153064.

8 J. Jakab, B. Miškić, Š. Mikšić, B. Juranić, V. Čosić, D. Schwarz and A. Včev, Adipogenesis as a Potential Anti-Obesity Target: A Review of Pharmacological Treatment and Natural Products, *Diabetes, Metab. Syndr. Obes.*, 2021, **14**, 67–83.

9 C. Saponaro, M. Gaggini, F. Carli and A. Gastaldelli, The Subtle Balance between Lipolysis and Lipogenesis: A Critical Point in Metabolic Homeostasis, *Nutrients*, 2015, **7**, 9453–9474.

10 G. F. Grabner, H. Xie, M. Schweiger and R. Zechner, Lipolysis: cellular mechanisms for lipid mobilization from fat stores, *Nat. Metab.*, 2021, **3**, 1445–1465.

11 J. Pagnon, M. Matzaris, R. Stark, R. C. R. Meex, S. L. Macaulay, W. Brown, P. E. O'Brien, T. Tiganis and M. J. Watt, Identification and Functional Characterization of Protein Kinase A Phosphorylation Sites in the Major Lipolytic Protein, Adipose Triglyceride Lipase, *Endocrinology*, 2012, **153**, 4278–4289.

12 E. London, M. Bloyd and C. A. Stratakis, PKA functions in metabolism and resistance to obesity: lessons from mouse and human studies, *J. Endocrinol.*, 2020, **246**, R51–R64.

13 T. S. Nielsen, N. Jessen, J. O. L. Jørgensen, N. Møller and S. Lund, Dissecting adipose tissue lipolysis: molecular regulation and implications for metabolic disease, *J. Mol. Endocrinol.*, 2014, **52**, R199–R222.

14 R. E. Duncan, M. Ahmadian, K. Jaworski, E. Sarkadi-Nagy and H. S. Sul, Regulation of lipolysis in adipocytes, *Annu. Rev. Nutr.*, 2007, **27**, 79–101.

15 M. Calderon-Dominguez, J. F. Mir, R. Fucho, M. Weber, D. Serra and L. Herrero, Fatty acid metabolism and the basis of brown adipose tissue function, *Adipocyte*, 2015, **5**, 98–118.

16 A. C. Carpentier, D. P. Blondin, K. A. Virtanen, D. Richard, F. Haman and É. E. Turcotte, Brown Adipose Tissue Energy Metabolism in Humans, *Front. Endocrinol.*, 2018, **9**, 447–447.

17 D. Ricquier, Uncoupling protein 1 of brown adipocytes, the only uncoupler: a historical perspective, *Front. Endocrinol.*, 2011, **2**, 85–85.

18 C. Porter, Quantification of UCP1 function in human brown adipose tissue, *Adipocyte*, 2017, **6**, 167–174.

19 A. Tsubota, Y. Okamatsu-Ogura, J. V. Bariuan, J. Mae, S. Matsuoka, J. Nio-Kobayashi and K. Kimura, Role of brown adipose tissue in body temperature control during the early postnatal period in Syrian hamsters and mice, *J. Vet. Med. Sci.*, 2019, **81**, 1461–1467.

20 A. Park, W. K. Kim and K.-H. Bae, Distinction of white, beige and brown adipocytes derived from mesenchymal stem cells, *World J. Stem Cells*, 2014, **6**, 33–42.

21 T. Imagaki, J. Sakai and S. Kajimura, Transcriptional and epigenetic control of brown and beige adipose cell fate and function, *Nat. Rev. Mol. Cell Biol.*, 2016, **17**, 480–495.

22 A. Kuryłowicz and M. Puzianowska-Kuźnicka, Induction of Adipose Tissue Browning as a Strategy to Combat Obesity, *Int. J. Mol. Sci.*, 2020, **21**(17), 6241.

23 M. Misra, Obesity pharmacotherapy: current perspectives and future directions, *Curr. Cardiol. Rev.*, 2013, **9**(1), 33–54.

24 K. Venkatakrishnan, H. F. Chiu and C. K. Wang, Extensive review of popular functional foods and nutraceuticals against obesity and its related complications with a special focus on randomized clinical trials, *Food Funct.*, 2019, **10**, 2313–2329.

25 N. Jain, R. Jain, V. Jain and S. J. P. Jain, A review on: Abelmoschus esculentus, *Pharmacia*, 2012, **1**(3), 84–89.

26 J. Messing, C. Thöle, M. Niehues, A. Shevtsova, E. Glocker, T. Borén and A. Hensel, Antiadhesive properties of Abelmoschus esculentus (Okra) immature fruit extract against Helicobacter pylori adhesion, *PLoS One*, 2014, **9**, e84836.

27 D. T. Wu, X. R. Nie, D. D. Shen, H. Y. Li, L. Zhao, Q. Zhang, D. R. Lin and W. Qin, Phenolic Compounds, Antioxidant Activities, and Inhibitory Effects on Digestive Enzymes of Different Cultivars of Okra (Abelmoschus esculentus), *Molecules*, 2020, **25**(6), 1276.

28 F. Xia, Y. Zhong, M. Li, Q. Chang, Y. Liao, X. Liu and R. Pan, Antioxidant and Anti-Fatigue Constituents of Okra, *Nutrients*, 2015, **7**, 8846–8858.

29 S. Fan, Y. Zhang, Q. Sun, L. Yu, M. Li, B. Zheng, X. Wu, B. Yang, Y. Li and C. Huang, Extract of okra lowers blood glucose and serum lipids in high-fat diet-induced obese C57BL/6 mice, *J. Nutr. Biochem.*, 2014, **25**, 702–709.

30 H. Wang, G. Chen, D. Ren and S. T. Yang, Hypolipidemic activity of okra is mediated through inhibition of lipogenesis and upregulation of cholesterol degradation, *Phytother. Res.*, 2014, **28**, 268–273.

31 V. Sabitha, S. Ramachandran, K. R. Naveen and K. Panneerselvam, Antidiabetic and antihyperlipidemic potential of Abelmoschus esculentus (L.) Moench. in streptozotocin-induced diabetic rats, *J. Pharm. BioAllied Sci.*, 2011, **3**, 397–402.



32 T. C. L. Bargut, V. Souza-Mello, M. B. Aguila and C. A. Mandarim-de-Lacerda, Browning of white adipose tissue: lessons from experimental models, *Horm. Mol. Biol. Clin. Invest.*, 2017, **31**(1), DOI: [10.1515/hmbci-2016-0051](https://doi.org/10.1515/hmbci-2016-0051).

33 H. Jin, K. Lee, S. Chei, H. J. Oh, K. P. Lee and B. Y. Lee, Ecklonia stolonifera Extract Suppresses Lipid Accumulation by Promoting Lipolysis and Adipose Browning in High-Fat Diet-Induced Obese Male Mice, *Cells*, 2020, **9**(4), 871.

34 B. L. Graf, I. Raskin, W. T. Cefalu and D. M. Ribnicky, Plant-derived therapeutics for the treatment of metabolic syndrome, *Curr. Opin. Invest. Drugs*, 2010, **11**, 1107–1115.

35 M. Boccellino and S. D'Angelo, Anti-Obesity Effects of Polyphenol Intake: Current Status and Future Possibilities, *Int. J. Mol. Sci.*, 2020, **21**, 5642.

36 M. Gao, Y. Ma and D. Liu, High-fat diet-induced adiposity, adipose inflammation, hepatic steatosis and hyperinsulinemia in outbred CD-1 mice, *PLoS One*, 2015, **10**(3), e0119784.

37 M. Longo, F. Zatterale, J. Naderi, L. Parrillo, P. Formisano, G. A. Raciti, F. Beguinot and C. Miele, Adipose Tissue Dysfunction as Determinant of Obesity-Associated Metabolic Complications, *Int. J. Mol. Sci.*, 2019, **20**, 2358.

38 D. Moseti, A. Regassa and W.-K. Kim, Molecular Regulation of Adipogenesis and Potential Anti-Adipogenic Bioactive Molecules, *Int. J. Mol. Sci.*, 2016, **17**, 124.

39 H. Jin, H.-J. Oh, J. Kim, K.-P. Lee, X. Han, O.-H. Lee and B.-Y. Lee, Effects of Ecklonia stolonifera extract on the obesity and skeletal muscle regeneration in high-fat diet-fed mice, *J. Funct. Foods*, 2021, **82**, 104511.

40 I. Romieu, L. Dossus, S. Barquera, H. M. Blotière, P. W. Franks, M. Gunter, N. Hwalla, S. D. Hursting, M. Leitzmann, B. Margetts, C. Nishida, N. Potischman, J. Seidell, M. Stepien, Y. Wang, K. Westerterp, P. Winichagoon, M. Wiseman and W. C. Willett, I. w. g. o. E. Balance and Obesity, Energy balance and obesity: what are the main drivers?, *Cancer, Causes Control*, 2017, **28**, 247–258.

41 M. C. Löffler, M. J. Betz, D. P. Blondin, R. Augustin, A. K. Sharma, Y.-H. Tseng, C. Scheele, H. Zimdahl, M. Mark, A. M. Hennige, C. Wolfrum, W. Langhans, B. S. Hamilton and H. Neubauer, Challenges in tackling energy expenditure as obesity therapy: From preclinical models to clinical application, *Mol. Metab.*, 2021, **51**, 101237.

42 S. H. Kim and J. Plutzky, Brown Fat and Browning for the Treatment of Obesity and Related Metabolic Disorders, *Diabetes Metab. J.*, 2016, **40**, 12–21.

43 L. Cheng, J. Wang, H. Dai, Y. Duan, Y. An, L. Shi, Y. Lv, H. Li, C. Wang, Q. Ma, Y. Li, P. Li, H. Du and B. Zhao, Brown and beige adipose tissue: a novel therapeutic strategy for obesity and type 2 diabetes mellitus, *Adipocyte*, 2021, **10**, 48–65.

44 G. Wade, A. McGahee, J. M. Ntambi and J. Simcox, Lipid Transport in Brown Adipocyte Thermogenesis, *Front. Physiol.*, 2021, **12**, 787535.

45 S. Larsson, H. A. Jones, O. Göransson, E. Degerman and C. Holm, Parathyroid hormone induces adipocyte lipolysis via PKA-mediated phosphorylation of hormone-sensitive lipase, *Cell. Signalling*, 2016, **28**, 204–213.

46 H. Jin, H.-J. Oh, S.-Y. Nah and B.-Y. Lee, Gintonin-enriched fraction protects against sarcopenic obesity by promoting energy expenditure and attenuating skeletal muscle atrophy in high-fat diet-fed mice, *J. Ginseng Res.*, 2022, **46**(3), 454–463.

47 D. Feng, J. Zou, D. Su, H. Mai, S. Zhang, P. Li and X. Zheng, Curcumin prevents high-fat diet-induced hepatic steatosis in ApoE(-/-) mice by improving intestinal barrier function and reducing endotoxin and liver TLR4/NF-κB inflammation, *Nutr. Metab.*, 2019, **16**, 79–79.

48 S. Morrison and S. L. McGee, 3T3-L1 adipocytes display phenotypic characteristics of multiple adipocyte lineages, *Adipocyte*, 2015, **4**, 295–302.

